Microelectronic Engineering 90 (2012) 152–154

Contents lists available at ScienceDirect

Microelectronic Engineering

journal homepage: www.elsevier.com/locate/mee

Optical modes of chiral photonic composites

A. Christofi [a,b,*], N. Stefanou [a], S. Thanos [b]

[a] University of Athens, Section of Solid State Physics, Panepistimioupolis, GR-157 84 Athens, Greece
[b] Institute of Materials Science, NCSR "Demokritos", GR-153 10 Athens, Greece

ARTICLE INFO

Article history:
Available online 1 April 2011

Keywords:
Photonic crystal
Chiral medium
Band structure
Band gap

ABSTRACT

We report on the eigenmodes of photonic crystals consisting of submicron homogeneous chiral spheres in a nonchiral isotropic medium, by means of full electrodynamic calculations using the layer-multiple-scattering method. It is shown that resonant modes of the individual spheres give rise to narrow bands that hybridize with the extended bands of the appropriate symmetry associated with light propagation in an underlying effective chiral medium. The resulting photonic dispersion diagram exhibits remarkable features, such as strong band bending away from the Bragg points with consequent negative-slope dispersion inside the first Brillouin zone and sizable frequency gaps specific to each polarization mode. We present a rigorous group-theory analysis to explain features of the calculated photonic band structure, peculiar to a system which possesses time-reversal but not space-inversion symmetry, and discuss some interesting aspects of the underlying physics.

Photonic crystals with chiral constituents have been investigated in relation to the occurrence of frequency band gaps [1]. More recently, it has been suggested that material chirality offers new opportunities to realize negative refraction and related effects in effectively uniform media. In particular, it has been shown that the existence of a chiral resonance, realized either in a mixture of small helical inclusions [2] or in an assembly of resonant particles in a nondispersive chiral medium [3], leads to negative refraction and superlensing for one polarization, resulting in improved and simplified designs of novel optical chiral metamaterials [4]. Furthermore, in the strong chirality regime, intriguing properties, such as chirality-dependent node switching, polarization-sensitive transmission, and handedness-dependent mode localization, have been reported on two-dimensional (2D) photonic structures consisting of infinite cylinders made of a chiral (meta)material in a dielectric background [5]. On the other hand, in photonic crystals formed by optically active constituents, the combined effect of space-inversion-symmetry breakdown and gyrotropy has the same impact on the eigenmode structure as the spin–orbit coupling in electronic band states, which allows one to draw certain parallels between electron spin and photospin transport in these periodic structures. Such an analysis was carried out on a 1D chiral/nonchiral periodic multilayer structure [6].

In the present communication we report a rigorous group-theory analysis to explain general features of the frequency band structure of 3D photonic crystals consisting of chiral spheres in a nonchiral (dielectric) medium and explain the physical origin of the different eigenmodes of the electromagnetic (EM) field in such structures.

The optical response of a homogeneous chiral material is described by the phenomenological Drude–Born–Fedorov constitutive relations [7]

$$\mathbf{D}(\mathbf{r},t) = \epsilon_c\epsilon_0[\mathbf{E}(\mathbf{r},t) + \beta_c\nabla\times\mathbf{E}(\mathbf{r},t)] \quad (1)$$

$$\mathbf{B}(\mathbf{r},t) = \mu_c\mu_0[\mathbf{H}(\mathbf{r},t) + \beta_c\nabla\times\mathbf{H}(\mathbf{r},t)], \quad (2)$$

where the dimensionless coefficients ϵ_c, μ_c correspond to the isotropic relative permittivity and permeability, respectively, while the chirality parameter β_c (in units of length) is a real number in the absence of dissipative losses. Homogeneous plane waves propagating in this material have the form of circularly polarized waves of either handedness with wave numbers $q_L = q_c/(1-q_c\beta_c)$ and $q_R = q_c/(1+q_c\beta_c)$, for left- and right-circular polarization, LCP and RCP, respectively, where $q_c = \omega\sqrt{\epsilon_c\mu_c}/c, c = 1/\sqrt{\epsilon_0\mu_0}$ being the velocity of light in vacuum.

When light is incident on a homogeneous chiral sphere of radius S, embedded in a nonchiral host medium characterized by ϵ and μ, a scattered field is generated. The expansion coefficients of the scattered field are obtained from those of the incident wave through the so-called scattering T matrix. We denote the matrix elements of $\mathbf{T}$ in the spherical-wave basis by $T_{Plm;P'l'm'}$, where P stands for the polarization mode, electric (E) or magnetic (H), and l, m are the usual angular momentum indices. Because of the spherical symmetry of the scatterer, $\mathbf{T}$ is diagonal in l and independent on m; however, it is not diagonal in P in the given representation, which reflects the mixing of the E and H modes upon

* Corresponding author at: University of Athens, Section of Solid State Physics, Panepistimioupolis, GR-157 84 Athens, Greece. Tel.: +30 210 727 6780.
E-mail address: aristi@ims.demokritos.gr (A. Christofi).

0167-9317/$ - see front matter © 2011 Elsevier B.V. All rights reserved.
doi:10.1016/j.mee.2011.03.019

scattering because of chirality. Therefore $T_{Plm;P'l'm'} = T_{PP';l}\,\delta_{ll'}\delta_{mm'}$. Closed-form expressions for $T_{PP';l}$ have been derived by Bohren [7].

The condition to have a scattered field in the absence of incident wave is satisfied at the poles of the T matrix and defines the eigenmodes of the particle. A chiral sphere in a dielectric environment does not support true bound states because the eigenvalues of the corresponding T matrix have no poles on the real-frequency axis. However, for each $l = 1, 2, \ldots$, one of the two eigenvalues of $\mathbf{T}$ has poles in the lower complex-frequency half-plane close to the real axis, at $\omega_{nl} - i\gamma_{nl}$, as $q_c\beta_c$ approaches unity. These poles correspond to 2^l-pole resonant modes of the EM field at ω_{nl} with inverse lifetime γ_{nl}.

We now consider an fcc crystal, with lattice constant a, of spheres embedded in a dielectric medium with $\epsilon = 3$ and $\mu = 1$. We view the crystal as a sequence of (001) crystallographic planes. In each plane the spheres are arranged on a square lattice, of lattice constant $a_0 = a\sqrt{2}/2$, while consecutive planes are separated by a distance $d = a/2$. The spheres have a radius $S = 0.45a_0$ and are made of a chiral material with $\epsilon_c = 2$, $\mu_c = 1$ and $\beta_c/a_0 = 0.2$. Assuming $\beta_c = 3 \times 10^{-8}$ m [5], $a_0 = 150$ nm. It is interesting to note that the given crystal lacks invariance under space inversion because of its chiral constituents. Therefore, the appropriate point symmetry group is O, which consists of only proper rotations, and not O_h that would be if the spheres were optically inactive [8].

We calculate the photonic band structure of this crystal by the layer-multiple-scattering method, which is well-established [9]. An advantage of the method in that it solves Maxwell equations in frequency domain and, therefore, it can treat dispersive materials, such as chiral substances, in a straightforward manner. The properties of the individual scatterers enter through the corresponding T matrix, and in-plane multiple scattering is evaluated in the spherical-wave basis using proper propagator functions. Subsequently, interlayer scattering is described in a plane-wave basis through appropriate transmission and reflection matrices. For a 3D crystal consisting of an infinite periodic sequence of planes of scatterers, stacked along the z direction, applying the Bloch condition for the wave field in the region between two consecutive unit layers leads to an eigenvalue equation, which gives the z component of the Bloch wave vector, k_z, for the given frequency ω and in-plane reduced wave vector component $\mathbf{k}_\parallel$. It turns out that, for given $\mathbf{k}_\parallel$ and ω, out of the eigenvalues $k_z(\omega, \mathbf{k}_\parallel)$ none or, at best, a few are real and the corresponding eigenvectors represent propagating modes of the EM field. The remaining eigenvalues $k_z(\omega, \mathbf{k}_\parallel)$ are complex and the corresponding eigenvectors represent evanescent waves. These have an amplitude which increases exponentially in the positive or negative z direction and, unlike the propagating waves, do not exist as physical entities in the infinite crystal. However, they are an essential part of the physical solutions in a slab of finite thickness. A region of frequency where propagating waves do not exist, for given $\mathbf{k}_\parallel$, constitutes a frequency gap of the EM field for the given $\mathbf{k}_\parallel$. In order to ensure adequate convergence in our calculations, we truncate the spherical-wave expansions at $l_{max} = 6$ and take into account 37 2D reciprocal lattice vectors in the relevant plane-wave expansions [9].

In Fig. 1 we display the calculated photonic band structure of the crystal under study along its [001] direction. The bands along this direction can be classified according to the irreducible representations (A, B, E_1, E_2) of the C_4 group, which is a subgroup of O [8]. All these bands are nondegenerate since the irreducible representations of C_4 are one dimensional. The E_1 and E_2 bands have the symmetry of LCP and RCP propagating waves, respectively, and thus can be excited by a wave of the appropriate polarization, incident normally on a finite (001) slab of the crystal. The A and B bands cannot be excited by an externally incident wave because they do not have the proper symmetry. These bands correspond to bound states of the EM field in a finite slab of the crystal and

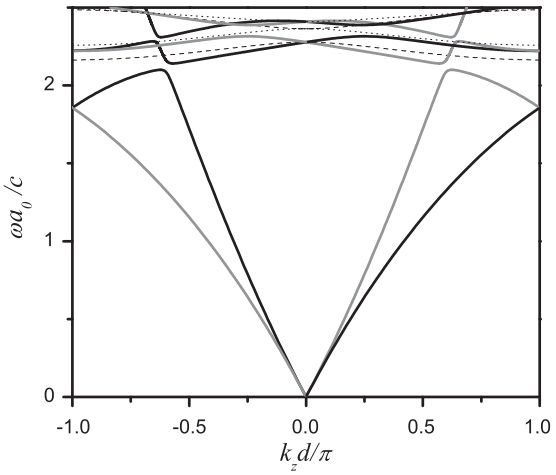

Fig. 1. The photonic band structure of the crystal under study, along its [001] direction. The bands of LCP and RCP eigenmodes are shown by black and gray solid lines, respectively. With dashed and dotted lines we denote inactive bands (see also Fig. 2).

decrease exponentially outside the slab on either side of it. To demonstrate this, we determined the eigenmodes of a (001) slab of the given crystal, consisting of $N_L = 4$ planes of spheres, for $\mathbf{k}_\parallel = (0, 0)$. Over the frequency range of each of these bands we obtain four eigenfrequencies which, plotted against values of the reduced wave number $k_z = n\pi/(N_L + 1)$, $n = 1, 2, \ldots, N_L, (N_L = 4)$, reproduce the corresponding dispersion curves of the infinite crystal as shown by the open circles in Fig. 2.

The eigenmodes at the center of the Brillouin zone, $\mathbf{k} = (0, 0, 0)$, have the symmetry of the full O point group, while at the boundaries of the Brillouin zone, $\mathbf{k} = (0, 0, \pm\pi/d)$, they have the symmetry of the D_4 point group, which is a subgroup of O. Compatibility between the irreducible representations of the O and C_4 and of the D_4 and C_4 groups (see Table 1) implies that the optically active LCP and RCP bands along the [001] direction, of E_1 and E_2 symmetry, respectively, converge to doubly degenerate modes of E symmetry at the corresponding boundaries of the Brillouin zone and

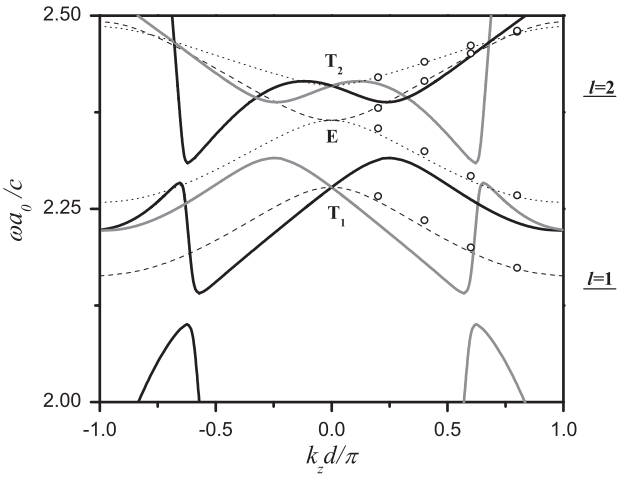

Fig. 2. A detail view of Fig. 1 over a limited frequency region about the lowest resonances of the single sphere, shown in the margin. The bands along the [001] direction have the symmetry of the C_4 group: A (dashed line), B (dotted line), E_1 (black solid line), E_2 (gray solid line). The eigenmodes at the center of the Brillouin zone are denoted by the corresponding irreducible representation of the appropriate point group, O. The open circles show the eigenfrequencies of a (001) slab of the given crystal, four-layers thick, plotted against discrete values of $k_z d/\pi = 1/5,\ 2/5,\ 3/5,\ 4/5$ (see text).

Table 1
Compatibility relations between the irreducible representations of the O and C_4, and of the D_4 and C_4 groups.

O	A_1	A_2	E	T_1	T_2
C_4	A	B	$A\,B$	$A\,E_1\,E_2$	$B\,E_1\,E_2$
D_4	A_1	B_1	A_2	B_2	E
C_4	A	B	A	B	E_1E_2

to three-fold degenerate (T_1 or T_2) modes at the center of the Brillouin zone, as shown in Fig. 2. Another interesting feature in the band diagram of Figs. 1 and 2 follows from invariance under time reversal, which reflects reciprocity as in the case of nonchiral photonic crystals: though $\omega_{nE_1}(\mathbf{k}) \neq \omega_{nE_1}(-\mathbf{k})$ and $\omega_{nE_2}(\mathbf{k}) \neq \omega_{nE_2}(-\mathbf{k})$, because of the lack of space-inversion symmetry, $\omega_{nE_1}(\mathbf{k}) = \omega_{nE_2}\ (-\mathbf{k})$, where $n = 1, 2, \ldots$ is a band index. We note that polarization selectivity and existence of optically inactive bands apply along high-symmetry directions, such as [001] or [111]. Along an arbitrary direction, all bands belong to the identity representation and thus can be excited by an appropriately incident wave of any polarization.

At low frequencies (below $\omega a_0/c \approx 2$) we obtain nondegenerate extended bands of LCP and RCP modes, of E_1 and E_2 symmetry, respectively, as expected for propagation in a homogeneous chiral effective medium, in the reduced zone representation because of structure periodicity. At higher frequencies, the dispersion diagram is characterized by narrow bands, which originate from the resonant modes of the individual spheres, weakly interacting between them. The E_1 and E_2 components of these resonance bands interact with the extended effective-medium bands of the same symmetry to produce the band structure shown in Figs. 1 and 2. It can be seen that frequency gaps open up as a result of anticrossing interactions, with consequent strong band bending and negative-slope dispersion inside the Brillouin zone. We note that the total number of bands shown in Fig. 1 equals the number expected from the interaction of the resonance bands with the "would be" extended effective-medium bands. For example, as can be seen in Fig. 2, the dipole resonances of the individual spheres give a threefold degenerate mode of T_1 symmetry at the center of the Brillouin zone, which is separated into an E_1, an E_2, and an A band along the [001] direction. Correspondingly, the quadrupole resonances give a threefold degenerate T_2 mode and a doubly degenerate E mode at $\mathbf{k} = (0, 0, 0)$. These are separated into an E_1, an E_2, and a B band and into an A and a B band along the [001] direction, respectively.

In summary, our results show that the photonic band structure of 3D chiral/nonchiral periodic composites exhibits remarkable features that endow these crystals with functionalities such as negative refraction, polarization-dependent slow-light transport, photospin splitting and filtering.

Acknowledgement

A. Christofi was supported by NCSR "Demokritos" through a postgraduate fellowship.

References

[1] I.E. Psarobas, N. Stefanou, A. Modinos, J. Opt. Soc. Am. A 16 (1999) 343.
[2] S. Tretyakov, I. Nevedov, A. Sihvola, S. Maslovski, C. Simovski, J. Electromagn. Waves Appl. 17 (2003) 695.
[3] J.B. Pendry, Science 306 (2004) 1353.
[4] B. Wang, J. Zhou, T. Koschny, M. Kafesaki, C.M. Soukoulis, J. Opt. A: Pure Appl. Opt. 11 (2009) 114003.
[5] C. He, M.H. Lu, R.C. Yin, T. Fan, Y.F. Chen, J. Appl. Phys. 108 (2010) 073103.
[6] F. Jonsson, C. Flytzanis, Phys. Rev. Lett. 97 (2006) 193903.
[7] C.F. Bohren, Chem. Phys. Lett. 29 (1974) 458.
[8] J.F. Cornwell, Group Theory and Electronic Energy Bands in Solids, North-Holland, Amsterdam, 1969.
[9] N. Stefanou, V. Yannopapas, A. Modinos, Comput. Phys. Commun. 132 (2000) 189.